Wavelength locking of single emitters and multi-emitter modules: Simulation & Experiments

Dan Yanson*, Noam Rappaport, Ophir Peleg, Yuri Berk, Nir Dahan,
Genady Klumel, Ilya Baskin, and Moshe Levy.

SCD – SemiConductor Devices, P.O.Box 2250/99, Haifa 31021, Israel

ABSTRACT

Wavelength-stabilized high-brightness single emitters are commonly used in fiber-coupled laser diode modules for pumping Yb-doped lasers at 976 nm, and Nd-doped ones at 808 nm. We investigate the spectral behavior of single emitters under wavelength-selective feedback from a volume Bragg (or hologram) grating (VBG) in a multi-emitter module.

By integrating a full VBG model as a multi-layer thin film structure with commercial raytracing software, we simulated wavelength locking conditions as a function of beam divergence and angular alignment tolerances. Good correlation between the simulated VBG feedback strength and experimentally measured locking ranges, in both VBG misalignment angle and laser temperature, is demonstrated.

The challenges of assembling multi-emitter modules based on beam-stacked optical architectures are specifically addressed, where the wavelength locking conditions must be achieved simultaneously with high fiber coupling efficiency for each emitter in the module. It is shown that angular misorientation between fast and slow-axis collimating optics can have a dramatic effect on the spectral and power performance of the module.

We report the development of our NEON-S wavelength-stabilized fiber laser pump module, which uses a VBG to provide wavelength-selective optical feedback in the collimated portion of the beam. Powered by our purpose-developed high-brightness single emitters, the module delivers 47 W output at 11 A from an 0.15 NA fiber and a 0.3 nm linewidth at 976 nm. Preliminary wavelength-locking results at 808 nm are also presented.

Keywords: laser diode, high-power laser, fiber coupled emitter, multi-emitter module, brightness, fiber laser pump, slow axis divergence, wavelength locking, frequency locking, wavelength stabilization, VBG, VHG, volume Bragg grating fiber coupling.

1. INTRODUCTION

Continuing advances in the fiber laser pumping market place ever-increasing demands on laser diode pumps [1]. Besides wattage, fiber laser makers often require that pump light be delivered with most of the energy concentrated in the narrow Yb absorption band at 976 nm [2]. In solid state laser pumping, Nd / Nd:YVO_4 crystals can be most efficiently pumped by laser diodes spectrally narrowed and locked at 808 nm.

These requirements are nearly impossible to meet with free-running high-power laser diodes, since they typically exhibit lasing spectra that are several nanometers wide. Worse still, their emission wavelength is a strong function of p-n junction temperature and undergoes a red-shift at a rate of 0.3 – 0.4 nm/K. Both the spectral linewidth and thermal wavelength drift issues can be successfully solved by optically locking a laser diode to a spectrally selective feedback element such as a Volume Bragg grating (VBG), aka Volume Holographic grating (VHG).

If placed in a collimated portion of the beam, a VBG will form an external cavity wherein the laser will lock to the VBG-defined wavelength favoring the lowest round-trip loss. In this configuration, a VBG reflectivity of 4% - 10% is sufficient to lock a laser diode with the front facet reflectivity chosen to meet both lockability and reliability considerations [3]. It does, however, require a high VBG alignment accuracy (typically <3 mrad) to couple the diffracted light back into the laser facet.

Alternatively, the VBG can be placed in an uncollimated, or partially collimated portion of the beam, where a higher VBG reflectivity is required for locking with a corresponding decrease in the laser efficiency, and more forgiving alignment tolerances can be afforded.

VBG wavelength locking has become a viable commercial technology and is deployed in various laser formats such as bars and stacks, reaching kilowatt powers [4], [5], [6]. It is also an enabling technology for high-power spectral beam combining [7], where the spatial brightness of multiple wavelength-locked laser sources can be scaled up at the expense of spectral brightness (i.e., total spectral bandwidth of the combined sources).

In this paper, we will address the wavelength locking of multi-emitter fiber-coupled laser diode modules commonly used for fiber laser pumping [4], [7], [8]. In this application, each of the single emitters in the module must be both coupled into the delivery fiber and wavelength-locked at the same time. The combination of high fiber coupling efficiency and strong VBG locking requirements presents additional challenges in the design and manufacturing of such modules. It is an object of this paper to analyze the wavelength locking requirements for single emitter devices and share some of the insights we gained in the process of integrating them in our fiber-coupled products.

At SCD, we have developed multi-emitter fiber coupled modules, named NEON, that deliver 50 W output from a 105 µm core, 0.15 NA fiber at 9xx nm wavelengths. While key aspects of the emitter and module development have been reported elsewhere [9], here we present the work on the simulation and characterization of a wavelength-stabilized version of the module by the name of NEON-S.

The paper is organized as follows: we start off by presenting the VBG model used in our simulations of wavelength-selective feedback into single emitters in Sec. 2. Then, in Sec. 3, we describe the single emitters we developed and their wavelength stabilization by a VBG element as standalone devices. In Sec. 4, we address the integration of these emitters into a fiber-coupled NEON module and present the device performance at 976 nm and 808 nm before we summarize with conclusions in Sec. 5.

2. SIMULATION

2.1 VBG model

A VBG (or VHG) is a holographic element containing planar refractive index modulation within a slab of photo-thermo-refractive glass. A careful optimization of slab thickness (typically 1 – 3 mm) and index modulation (10^{-4} – 10^{-5}) within the host glass allows a desired diffraction efficiency and linewidth (typically < 0.5 nm FWHM) to be engineered.

In this work, we employed a commercial optical engineering package, FRED by Photon Engineering LLC, to realize a full VBG model as a multi-layer thin film structure of some 5,000 layers. The VBG element was set up as a glass slab incorporating a thin-film coating of repeated stacks of high/low index layer pairs. We first calibrated the model by using an ideal plane wave source against the characterization data provided by the VBG manufacturer (OptiGrate Inc.). Both the spectral bandwidth and diffraction efficiency were replicated with very good agreement as demonstrated by Figure 1(a).

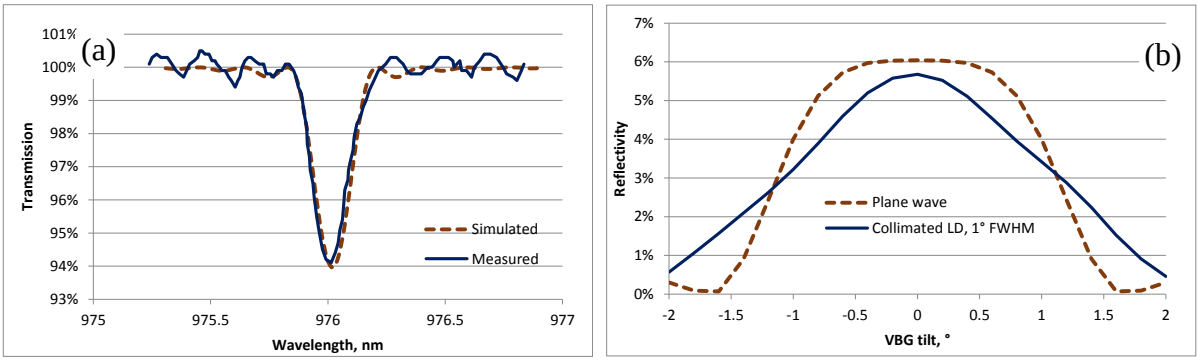

Figure 1. (a) Simulated (raytracing) and measured (manufacturer's data) transmission spectra for a VBG at normal incidence. (b) Simulated VBG reflectivity at a diffraction wavelength of 976 nm as a function of VBG tilt for an ideal plane wave source (dashed brown curve) and a collimated laser diode (1° slow axis divergence, solid blue curve).

We then evaluated the effect of using realistic laser diode beams, where the collimation quality in the slow axis can be quite poor due to the highly multimode nature of the beam (M^2 ~ 20 – 30). For comparison, we juxtaposed a poorly collimated beam having a 1° FWHM divergence with an ideal plane wave, both at a peak diffraction wavelength of 976 nm. The FRED software allowed key design parameters (e.g., the VBG tilt, source wavelength, and divergence) to be scanned by using a powerful script language. In Figure 1(b), we simulated the diffraction efficiency of a 6% VBG as a function of its angular tilt for both sources. It can be seen that not only does the multimode beam fail to reach the peak diffraction efficiency of 6%, but its diffraction efficiency falls off faster with VBG tilt, i.e., it offers no plateau at around normal incidence as opposed to that exhibited by the plane wave source. This effect both increases the sensitivity of VBG alignment in the multimode slow axis of a broad-area laser diode such as the single emitter and places certain requirements on the collimating optics.

2.2 Single emitter under VBG feedback

We used the FRED VBG model to investigate the amount of feedback received by a single emitter, with the VBG providing wavelength-selective optical feedback in the collimated portion of the beam. The VBG model was introduced into a raytracing model of a 95 µm-wide single emitter comprising fast-axis (FAC) and slow-axis (SAC) collimators as depicted in Figure 2(a). The effective focal lengths of the FAC and SAC were 0.5 mm and 9 mm, respectively. The model allowed us to investigate the VBG feedback strength as a function of several parameters, including the VBG misalignment in both fast and slow axes.

We found that, under ideal alignment and locking conditions, the feedback coupling efficiency into the facet is around 80% (4.7% of the total power for a 6% VBG reflectance) as can be seen in Figure 2(b). Note that our raytracing model cannot provide information on how much of the power incident on the laser diode facet is actually coupled into the epitaxial waveguide, or what lasing modes are excited.

Predictably, the VBG angular tolerance was found to be different for the fast and slow axes, with the feedback level exhibiting much higher sensitivity to vertical (fast-axis) VBG tilt. The sensitivity difference is due to the epitaxial waveguide only being ~1.5 µm thick as opposed to 95 µm wide, and the focal lengths of the collimating optics involved. In Figure 2(b), one can see that the feedback remains above 3.5% over a vertical (fast-axis) VBG tilt of ±0.7 mrad, which was found to be in good agreement with experimental results (the solid arrows showing the locking ranges observed) as will be explained in Sec. 3.2. In the slow axis, the VBG tilt range with feedback >3.5% is approximately double that in the fast axis, at ±1.4 mrad, which suggests that the VBG alignment in the fast axis is twice as sensitive as in the slow axis.

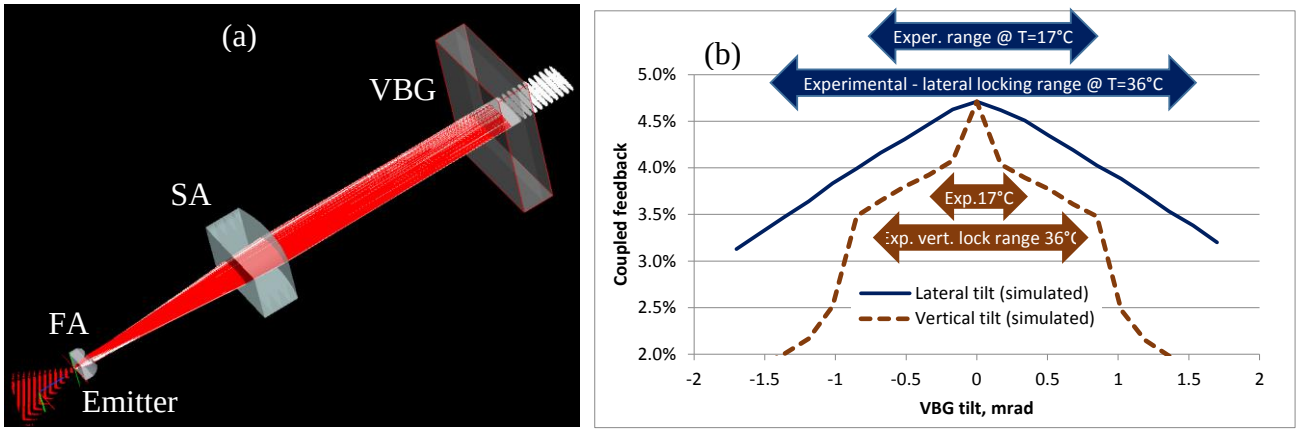

Figure 2. (a) Raytracing model used in FRED simulation: white rays originate from emitter source, red rays from VBG diffraction. (b) VBG feedback coupled into emitter facet as percentage of output power vs. VBG tilt in two axes. The blue arrows indicate experimentally measured locking limits in lateral VBG tilt, brown arrows in vertical VBG tilt, both for emitter temperatures of 17 and 36°C.

3. SINGLE EMITTER EXPERIMENTS

3.1 Single emitters

For use in our fiber-coupled products, we have developed a common Al-based epitaxial platform utilizing an asymmetric structure design, with only minor changes to the InGaAs quantum well (QW) com,position and position to allow for wavelength adjustment. By using an asymmetric waveguide structure, we reported [9] a very low optical loss of under 0.5 cm^{-1} enabling wall-plug efficiencies (WPE) in excess of 60%. Another feature of the epitaxial design was a low overlap integral of the optical mode with the quantum well, which allowed a reduced far-field divergence in the slow axis (<14° full angle at $1/e^2$ level) [10].

Wafers with different photoluminescence wavelengths earmarked for lasing at 970 - 980 nm were processed into single emitters with a 95 µm lateral emission aperture (for compatibility with fiber coupling) and a 4 mm cavity. The lasers incorporated a current block region at either facet, where current injection was suppressed with a view to minimizing the free carrier absorption in this critical region. After cleaving, the chip facets were treated with our laser mirror passivation process [11] and coated with AR / HR coatings. Finally, the devices were assembled onto ceramic carriers and wirebonded.

At heatsink temperature T_h = 25°C under 12 A CW pumping, these devices reach or exceed an average power of 11 W, with light-current (*L-I*) characteristics shown in Figure 3(a). Note that while the devices can be driven to 20 A, they are qualified for 12 A operation [12] with a mean time to failure (MTTF) of over 340k hours. A typical free-running spectrum of a single emitter at T_h = 25°C is shown in Figure 3(b), with a peak wavelength at 970 nm.

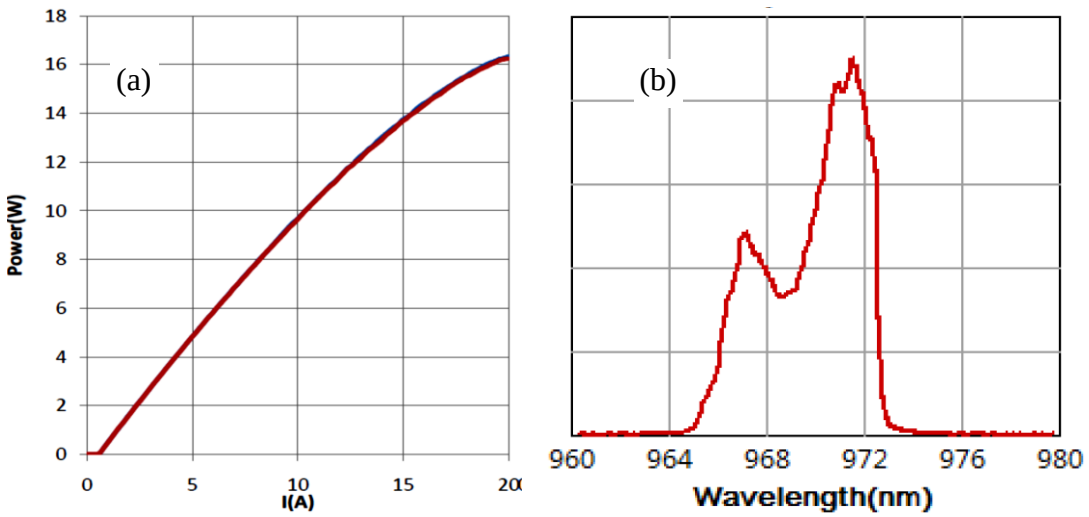

Figure 3. (a)Typical light-current characteristics of single emitters; (b) spectrum at 12A current and heatsink T = 25°C.

3.2 Wavelength locking limits

To investigate the wavelength locking limits of our single emitters, we used devices fabricated from wafers at the extremes of the operational wavelength range. In what follows, we will refer to devices from blue-shifted Wafer **B** with a free-running wavelength at around 968 nm, and red-shifted Wafer **R** at around 982 nm, both at 12 A CW operation and a heatsink temperature of T_h = 25°C, with an estimated junction temperature T_j = 45°C. Their representative spectra are shown on a logarithmic scale in Figure 4(a).

Single emitters from both Wafers **B** and **R** were packaged and collimated according to the setup of Figure 2(a) with a VBG having a diffraction efficiency of 6%. The setup offered temperature control and operation in either CW or QCW mode.

It can be seen from Figure 4(a) that at T_h = 25°C, a typical device from Wafer **B** has no spontaneous emission (and hence little or no optical gain) at the VBG wavelength of 976 nm even at the noise floor, which is some 40 dB down from the

peak intensity. Therefore, it is unsurprising that no wavelength locking was achieved at that temperature, and the spectrum under VBG feedback [solid blue curve in Figure 4(b)] exhibits no line at 976 nm. However, when the device was heated to T_h = 36°C (estimated T_j = 57°C) causing the gain peak to red-shift by about 4 nm, VBG locking was obtained as can be seen from the spectrum of Figure 4(b) (dotted red line). Even then, the locking was rather weak with a side-mode suppression ratio of less than 20 dB. This suggests that the Wafer **B** devices are too blue-shifted for VBG-locked operation even at elevated temperatures.

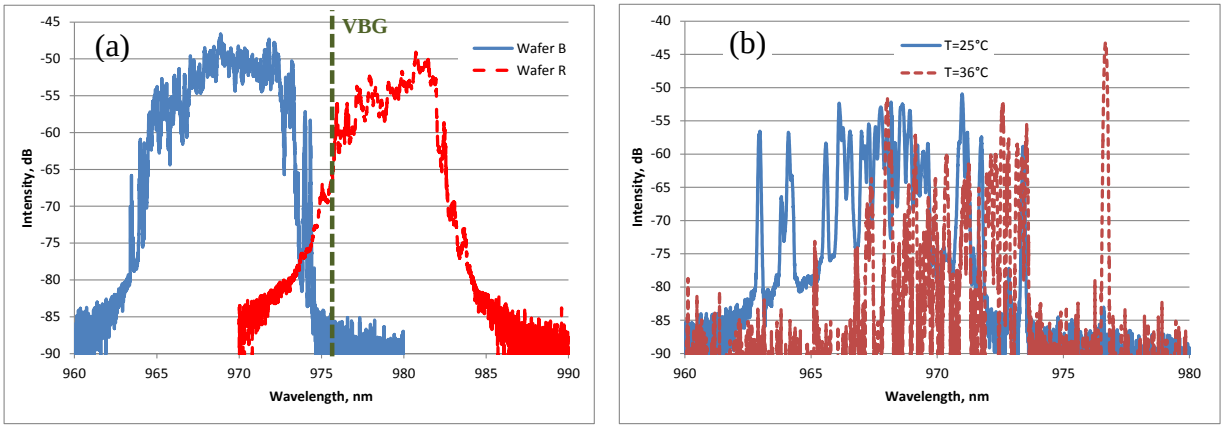

Figure 4. (a) Free-running spectra of emitters from Wafers **B** & **R** at I=11A CW current and heatsink temperature T_h =25°C. (b) Spectra of emitter from Wafer **B** under VBG feedback at I=11A CW for two temperatures T_h =25 and 36°C.

By contrast, Wafer **R** devices were quite amenable to VBG locking at T_h = 25°C, which is consistent with the fact the material offers sufficient gain (within 10 dB of the peak) at 976 nm according to from Figure 4(a). At the same time, the locking disappeared at the elevated temperature T_h = 36°C.

Based on the performance of Wafer **B** and **R** devices, we can conclude that VBG locking can be achieved for a free-running peak wavelength that is up to some 6 nm from the VBG line on either blue or red side. This would correspond to a locking range of up to 40°C in heatsink temperature. Indeed, for a device from a different wafer that was optimized for 976 nm lasing, we observed full locking across the 17 - 45°C temperature range (setup limited).

Another important consideration is the difference in the junction temperature T_j between CW and QCW operation. While most high-power fiber-coupled laser diode products are operated in CW mode, their active alignment and optical assembly are performed in QCW mode to prevent damage to packaging and fiber. In QCW mode, the junction temperature T_j is assumed to be identical to the heatsink one, $T_j \approx T_h$, whereas in CW mode T_j is substantially higher than T_h (by about 20°C in our NEON module). Therefore, for VBG and optics assembly in QCW mode, either heating is required to bring T_j close it its CW value, or the emitter lockability range should cover both QCW and CW conditions.

To explore the angular locking range, we used a Wafer **R** device in QCW mode, where free-running lasing was tuned to 976 nm by heating the device to T_h = 36°C. Under these conditions, the VBG feedback coincides with peak spectral gain, and the laser is expected to exhibit the broadest angular locking range. Indeed, as shown in solid arrows in Figure 2(b) earlier, a vertical (fast-axis) VBG tilt range of ±0.8 mrad, and a horizontal (slow-axis) one of ±1.5 mrad, were measured, which are both nearly identical to the simulated values.

On cooling the device to T_h = 17°C, the peak spectral gain was blue-shifted by some 6 nm pushing the laser to its lockability limit, with the angular locking range greatly reduced to ±0.25 mrad and ±0.8 mrad in the fast and slow axes, respectively [see the solid arrows in Figure 2(b)]. This behavior is consistent with the fact that the laser requires a higher feedback level to remain locked when its peak spectral gain is detuned from the VBG wavelength.

Furthermore, we observed a change in the emitter power between locked and unlocked conditions, the latter obtained by keeping the VBG in the laser beam but twisting it significantly out of alignment, and all other parameters, such as current and temperature, kept constant. In devices with ultralow AR coated facets (<0.1% estimated), the locked power could be as much as 20% higher than in an unlocked case. With somewhat higher facet reflectivity so as to mitigate the risk of feedback-related catastrophic facet failure [3], the locked power would be very similar to the unlocked one, which is

consistent with Ref. [4], or slightly lower, but by no more than 6% corresponding to the power fraction diffracted by the VBG. [3]In all cases, the highest locked power was obtained at a position where the spectral gain peak matched the VBG wavelength.

4. MULTI-EMITTER FIBER-COUPLED MODULE

4.1 Multi-emitter module assembly

In this section, we address the optical alignment and assembly of multi-emitter modules based on beam-stacked optical architectures, where a common VBG is placed to wavelength-lock all emitters together. In this case, the wavelength locking conditions must be achieved simultaneously with high fiber coupling efficiency for each emitter in the module. Furthermore, different emitters in the module may have different thermal dissipation paths and therefore operate at different junction temperatures T_j. The specifications for our NEON-S product dictate that the laser emission remains locked over a base temperature range of 20 – 30°C, with >90% of the power contained within a spectral window of 974.5 – 977 nm. The combination of these requirements, collectively for all emitters, makes the manufacturing of such modules particularly challenging.

The demanding angular tolerances of VBG alignment (<1.5 mrad full range in the fast axis for each emitter in our case) are comparable to, or even tighter than, the beam pointing tolerances required for high fiber coupling efficiency. Worse yet, collimation errors may degrade the feedback level provided by the VBG and thus exacerbate the angular sensitivity.

It is not surprising, then, that we only succeeded in partially locking our NEON-S module prototypes when we introduced the VBG at the end of the assembly process. With all the emitters and optics assembled to achieve a maximum fiber coupling efficiency, we performed VBG alignment as a final assembly step only to discover that the emitters could only be locked individually, or in groups, but no single VBG orientation would lock all the emitters simultaneously with sufficient side-mode suppression ratio. It was often the case that, for a particular VBG placement, some emitters were at the edge of their angular locking ranges, causing them to lose locking even with a small change in temperature.

We established that the alignment conditions for the collimating elements, such as the FAC and SAC, differed for maximum fiber-coupled power and maximum locking criteria. In other words, there was a trade-off between the best fiber coupling efficiency and wavelength locking to be made in the assembly of emitter collimating optics.

To address the issue, we performed extensive simulations by integrating the VBG model of Figure 2(a) into the full raytracing model of our NEON-S module and observing the effect of various alignment errors on the discrepancy between best fiber coupling and best locking conditions. While most errors would cause a simultaneous reduction in both the fiber coupling and locking feedback, two types of angular misalignment were identified that would cause a discrepancy between the two criteria:

1. Misalignment between the fiber focusing optics and the geometrical axis of the module that defines the emitter placement;
2. Cross-talk (non-orthogonality) between the fast and slow axes in the emitter collimating optics, i.e., angular twist about the beam axis of either the FAC or SAC element.

We illustrate a misalignment of type 2 above in Figure 5(a), where we simulate the optical alignment of a FAC with a VBG already in place. Under ideal alignment, both the peak fiber efficiency of 93% (solid blue curve) and peak VBG feedback level of 4.9% (dashed brown line) occur at the nominal FAC position (0 µm defocus). The graph illustrates that a 1° angular misorientation of the optical axis of the SAC can cause not only a reduction both in the coupling efficiency and the peak VBG feedback strength, but a mismatch between the two in terms of the FAC position. This type of error would cause the best fiber coupling to be achieved at a FAC defocus of up to 1 µm, whereas the best locking would be achieved at a defocus beyond 2 µm from nominal alignment.

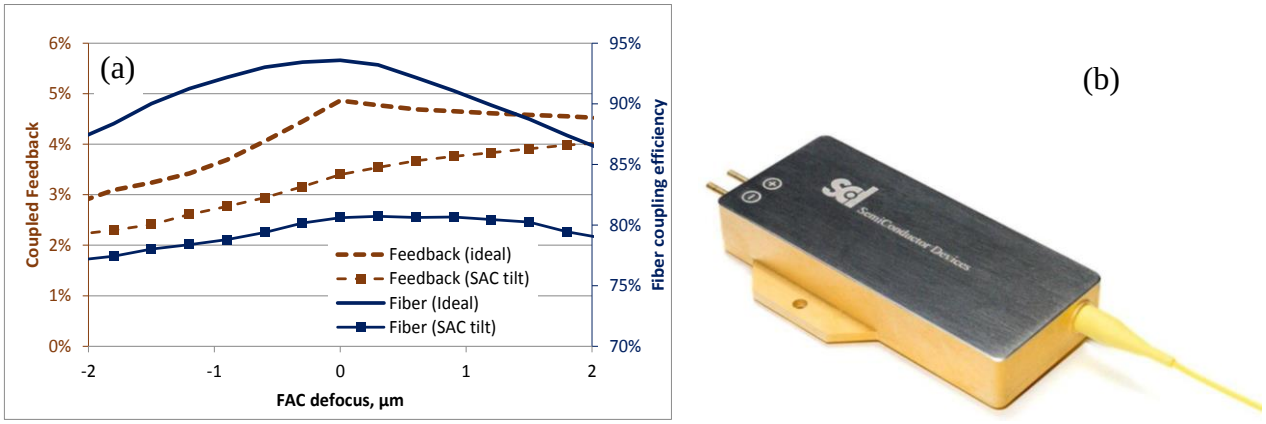

Figure 5. (a) Optical alignment simulation of VBG feedback and fiber coupling efficiency for ideal and misaligned cases. (b) Multi-emitter NEON-S module at 976nm.

By taking extra care to ensure the parallelism of the FAC element to the p-n junction of the laser, and orthogonality of the optical axis of the SAC element, we have been able to solve the assembly issues and commence the manufacturing of our NEON-S product shown in Figure 5(b).

We also observed the effect of improved collimation on the fiber launch in the NEON-S multi-emitter modules. By characterizing the far-field patterns of coupled laser emission emerging from the 0.15 NA delivery fiber, we compute the angular filling of the fiber as the fraction of the total energy contained within a certain numerical aperture (NA). From the angular distributions of Figure 6, one can observe a tighter angular spread of emission in VBG-locked modules with collimation correction than in non-stabilized modules that were assembled for highest coupled power alone. The latter contain some energy propagating in the cladding at high angles excess of the fiber NA, which is highly undesirable due to the resulting heating and possibly burning of the polymer buffer coating on the fiber.

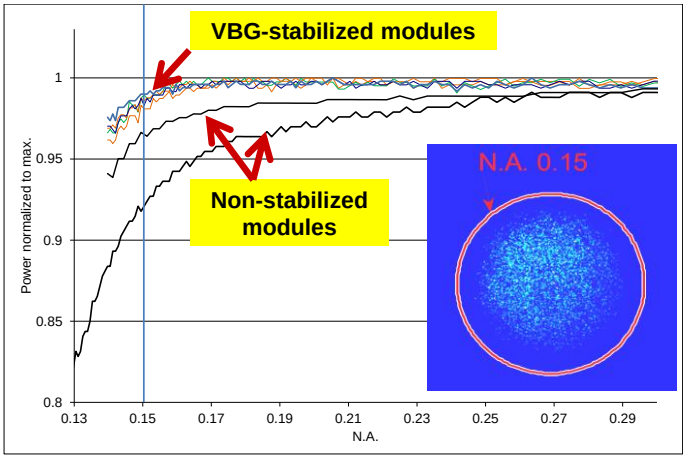

Figure 6. Angular filling of power in 0.15 NA fiber characterized from far-field pattern (inset).

It should be emphasized that the enhanced power confinement in VBG-stabilized modules comes from the improved emitter collimation and tighter alignment tolerances to achieve maximum locking, rather than from any direct VBG effects.

4.2 Module performance at 976nm

We have completed the development of our wavelength-stabilized NEON-S module for Yb fiber laser pumping at 975.6 nm. The module incorporates purpose-developed single emitters, both in terms of wavelength adjustment for optical locking over the operating temperature range, and an appropriate AR coating on the front facet to increase their sensitivity to external feedback whilst mitigating the risk of feedback-related catastrophic facet failure.

The module remains wavelength-locked at 976 nm over base temperatures of 20 – 30°C at an 11 A drive current, with the spectral linewidth narrowed to 0.3 nm FWHM as shown in Figure 7(b). The NEON-S module produces 47 W output within its locking range [Figure 7(a)], which is delivered via a 105 µm core, 0.15 NA fiber.

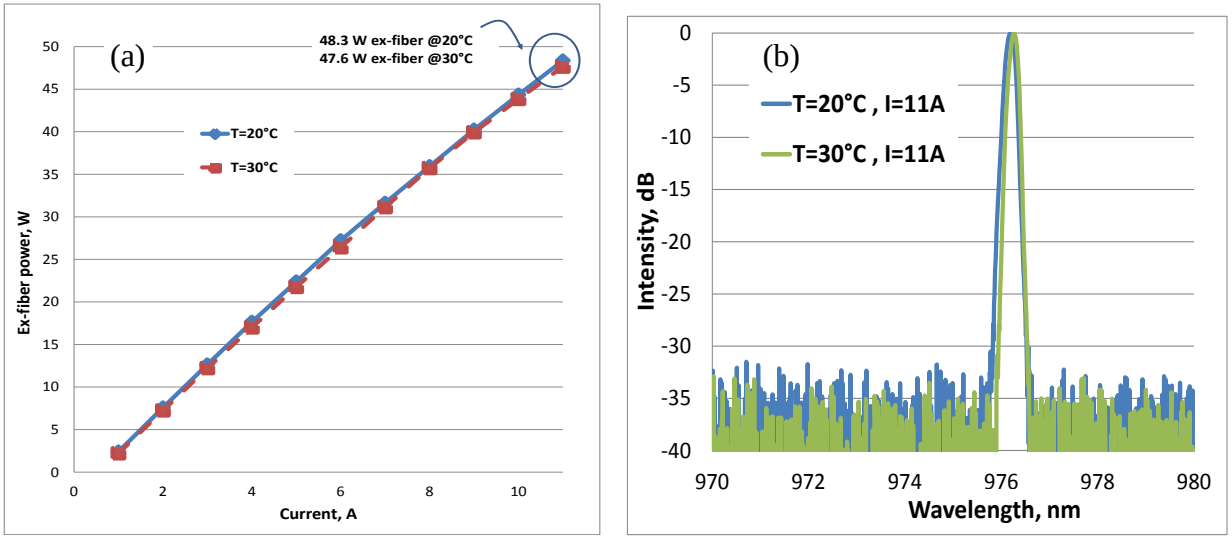

Figure 7. Light-current characteristics (a) and spectra (b) of a wavelength-stabilized NEON-S module at two different temperatures (20°C and 30°C).

4.3 Module development at 808nm

We are also completing the development of a wavelength-stabilized fiber-coupled module for pumping Nd:YVO_4 crystals at a wavelength of 808 nm. The module is powered by single emitters each delivering 7 W at a current of 8 A at a heatsink temperature T_h = 25°C.

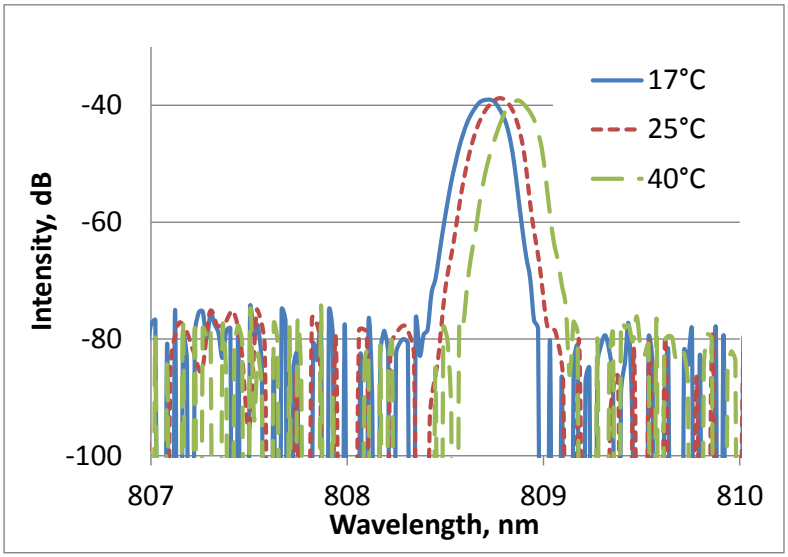

Figure 8. Spectra of a wavelength-stabilized 808nm module at 3 different base temperatures.

By applying the assembly process described in Sec.4.1, we have achieved excellent wavelength locking to a VBG at 808.5 nm with an out-of-band power suppression of >40 dB (noise limited) over base temperatures from 17°C to 40°C, as demonstrated in Figure 8. The total spectral drift was only ~0.3nm over 23 degrees and probably comes from the thermal shift within the VBG itself.

5. CONCLUSIONS

We have carried out simulation and experimental studies of the wavelength locking of high-power single emitters using a volume Bragg grating element to provide wavelength-selective optical feedback in the collimated portion of the beam. Our external cavity VBG model built using the FRED optical engineering software enabled us to make reliable predictions of the angular alignment tolerances in agreement with experimental results.

The VBG locking range and alignment tolerances were found to be a strong function of the peak gain wavelength of the laser under the operating conditions (temperature, current, CW/QCW mode).

We established that careful spectral engineering is required to ensure emitter locking within the full range of operating conditions in CW mode as well as under optical assembly conditions in QCW mode.

We also shared useful insights into the assembly of multi-emitter fiber-coupled pump modules with wavelength stabilization. It was shown that, by avoiding collimation errors, emitters could be both collimated and wavelength-locked with high fiber-coupling efficiency. Special care must be taken to avoid optical cross-talk between the fast and slow axes of the collimating optics.

Finally, we reported the performance of our wavelength-stabilized NEON-S product that delivers 47 W output from a 105 µm core, 0.15 NA fiber at a 976 nm wavelength. Progress in wavelength locking at 808 nm over a broad temperature range is also reported.

ACKNOWLEDGEMENTS

The authors would like to thank A.Algali, S. Geva, M. Avisar, M. Blonder, and Z. Madar for their technical assistance with the fabrication, assembly and characterization of the laser devices presented here. We are also grateful to Ryan Irvin and Tom Davies of Photon Engineering LLC for their support and helpful advice on the VBG ray-racing model in the FRED application environment.

REFERENCES

[1] L. Vaissie, T. Steele, and P. Rudy. "High-power diode lasers advance pumping applications." *Laser Focus World* (June 2008).

[2] G. Steckman, L. Wenhai, R. Platz, D. Schroeder, C. Moser, F. Havermeyer, "Volume Holographic Grating Wavelength Stabilized Laser Diodes," *IEEE Journal Sel. Topics in Q. Elec.,* vol.13, no.3, pp.672-678, 2007; doi: 10.1109/JSTQE.2007.896060.

[3] B. Leonhäuser, H. Kissel, A. Unger, B. Köhler, and J. Biesenbach, "Feedback-induced catastrophic optical mirror damage (COMD) on 976nm broad area single emitters with different AR reflectivity", Proc. SPIE 8965, High-Power Diode Laser Technology and Applications XII, 896506 (March 7, 2014); doi:10.1117/12.2039153.

[4] P. Leisher, A. Brown, R. Martinsen, J. Haden, M. Reynolds, S. Lin, R. Renner, K. Kennedy "Wavelength stabilized diode laser based devices free of power or efficiency penalties", *Proc. SPIE 7918, High-Power Diode Laser Technology and Applications IX*, 79180D (22 February 2011); doi: 10.1117/12.876078

[5] B. Köhler, T. Brand, M. Haag, J. Biesenbach, "Wavelength stabilized high-power diode laser modules", *Proc. SPIE 7198, High-Power Diode Laser Technology and Applications VII,* 719810 (February 23, 2009); doi:10.1117/12.809541.

[6] B. Köhler, A. Unger, T. Kindervater, S. Drovs, P. Wolf, et al, "Wavelength stabilized multi-kW diode laser systems", *Proc. SPIE 9348, High-Power Diode Laser Technology and Applications XIII*, 93480Q (April 1, 2015); doi:10.1117/12.2079428.
[7] S. Heinemann; H. Fritsche; B. Kruschke, T. Schmidt and W. Gries, "Compact high brightness diode laser emitting 500W from a 100µm fiber ", *Proc. SPIE 8605, High-Power Diode Laser Technology and Applications XI*, 86050Q (February 26, 2013); doi:10.1117/12.2003299.
[8] S. Heinemann, B. Lewis, B. Regaard, and T. Schmidt, "Single emitter based diode lasers with high brightness high power and narrow linewidth," *Proc. SPIE 7918, High-Power Diode Laser Technology and Applications IX*, 79180M (February 21, 2011); doi:10.1117/12.871955.
[9] D. Yanson, M. Levy, O. Peleg, N. Rappaport, M. Shamay, et al, "Low-NA fiber laser pumps powered by high-brightness single emitters", *Proc. SPIE 9348, High-Power Diode Laser Technology and Applications XIII*, 934806 (March 13, 2015); doi:10.1117/12.2079422.
[10] D. Yanson, N. Rappaport, M. Shamay, S. Cohen, Yuri Berk, et al. "Brightness-enhanced high-efficiency single emitters for fiber laser pumping", *Proc. SPIE 8605, High-Power Diode Laser Technology and Applications XI*, 860505 (February 26, 2013); doi:10.1117/12.2003838.
[11] D. Yanson, M. Levy, M. Shamay, R. Tesler, N. Rappaport, Y. Don, Y. Karni, I. Schnitzer, N. Sicron, and S. Shusterman, "Facet engineering of high power single emitters," *Proc. SPIE 7918, High-Power Diode Laser Technology and Applications IX*, 79180Z (21 February 2011); doi: 10.1117/12.876261.
[12] D. Yanson, N. Rappaport, M. Shamay, S. Cohen, Yuri Berk, et al. "High-power single emitters for fiber laser pumping across 8xx nm – 9xx nm wavelength bands", Proc. SPIE 8241, High-Power Diode Laser Technology and Applications X, 82410A (February 9, 2012); doi:10.1117/12.909016.